Effect of Physical Properties of Softwoods on Embedment Strength Performance of Self-tapping Screws

In-Hwan Lee, and Keon-Ho Kim *

The embedment strength performance of the self-tapping screw (STS) connector, used as a cross-laminated timber fastener, was evaluated considering tree species' density and load direction as parameters. The STS had a diameter of 8, 10, and 12 mm. Considering the characteristics of the STS, the embedment strength of the threaded area and the shank area were compared. A larger diameter of the STS resulted in a higher yield load in all directions of the respective wood. The effective embedment area can estimate a more accurate value for the embedment strength. The embedment strength of the longitudinal cross section as the embedment area was higher than that of the radial and tangential sections. For the loading direction, the ratio of the embedment strength parallel and perpendicular to the grain of the specimens was 0.40 to 0.58 by wood species. The embedment strength predicted based on the specific gravity and diameter of the fastener differed considerably by 38% to 56% from the actual embedment strength of STS using the effective embedment area. This paper provides data for setting the adjustment factors predicting the embedment strength of STS connection.

DOI: 10.15376/biores.18.2.3576-3589

Keywords: Embedment strength; Softwood; Self-tapping screw; Yield load; Embedment direction

Contact information: Wood Engineering Division, Forest Products and Industry Department, National Institute of Forest Science, 57 Hoegi-ro, Dongdaemun-gu, Seoul 02455, Republic of Korea;
** Corresponding author: keon@korea.kr*

INTRODUCTION

With the development of engineering timber, such as glulam and cross-laminated timber (CLT), timber construction is being built in large dimensions and heights (Nguyen *et al.* 2018; van de Lindt *et al.* 2019; Aloisio *et al.* 2020). The height limit for wooden structures varies by country, but in Korea, the market for wooden structures, including CLT, is expected to expand due to the elimination of the size limit for wooden structures in 2020. Alternatively, wood products used for domestic timber construction are more dependent on imported goods than domestic goods. In 2020, the proportion of domestic wood use in Korea was 18.6%, which is insufficient compared to 74.8% constituted by imported wood and wood products. In particular, when used as a construction material, the proportion of domestic wood used is 11.3%, which is largely dependent on imports (Market Survey of Timber Products 2020). Therefore, research is needed to increase the demand for domestic timber.

Identifying the exact basic mechanical properties of tree species is one of the ways to increase the use of domestic timber. Korean softwood is classified into four groups according to its specific gravity, and the representative softwoods in each group are

Japanese larch, red pine, Korean pine, and Japanese cedar (Korea Forest Service 3020 2018). Looking at the purchase of softwood by Korean sawmill manufacturers, the most representative species are, in this order: Japanese larch 56.7%, red pine 33.2%, Korean pine 2.8%, cypress 1.6%, and Japanese cedar 1.5%. The joints of the wooden structures are one of the most vulnerable places where the load stress is concentrated under loading. Therefore, the design of joints is as important in structural design as the design of structural members. The joint is designed based on the bending strength of the fastener and the embedment strength of the structural member to predict the strength of the joint. The equation for predicting the joint strength is calculated using the European yield model (EYM) proposed by Johansen (1949). Various fasteners, such as drift pins, bolts, and nails, are used for timber construction, and the embedment strength of the fasteners is proposed as an experimental formula using the density of wood and diameter of fastener in each country (Diets *et al*. 2015; Brandner *et al*. 2019). Therefore, the use of native species is expected to increase when the load-embedment strength for representative tree species is verified in the native tree species. The load-embedment strength of pine, a representative tree species for softwoods, was examined in the previous study, and the need for more research in Korea was indicated (Lee *et al.* 2022). The pull-out resistance strength of timber is also important, and further research needs to be conducted.

Self-tapping screws (STSs) are widely used as fasteners for CLT connections because of their good performance and workability without any preparatory work (Jockwer *et al.* 2014; Dietsch and Brandner 2015; Brandner 2019; Khan *et al.* 2021; Mirdad *et al.* 2022). The mechanical performance and behavior of STS joints are being studied in several countries (Mohammad *et al.* 2018; Hossain *et al.* 2019; Brown *et al.* 2021; Fitzgerald *et al.* 2021; Li *et al*. 2021; Xu *et al*. 2021). It has been reported that the mechanical performance of the STS joint is correlated with the density of the structural timber.

This study investigated the embedment capacity of STS joints on structural timber (CLT) for different tree species. Considering the connection method, the embedment strength was compared as a function of the embedment section according to the load direction, and the effect of STS shape on the embedment strength was investigated.

EXPERIMENTAL

Materials

For the test materials, Japanese larch (*Larix kaempferi* (Lamb.) Carriere) with specific gravity of 0.51, Korean pine (*Pinus koraiensis*) with specific gravity of 0.45, and Japanese cedar (*Cryptomeria japonica*) with specific gravity of 0.36 were used as the tree groups for softwood structural materials in Korea (Korea Forest Service 3020 2018). The test specimens were cut into 50 × 50 mm^2 sections.

Table 1. STS Codes and Dimensions

CODE	d_1	d_2	L	A	B	d_s	d_c	t_1	t_2
HBS8120	8	5.4	120	60	60	5.8	6.8	1.25	4
HBS10120	10	6.4	120	60	60	7	8.4	1.4	4.1
HBS12120	12	6.8	120	40	80	8	9	2.2	3.8

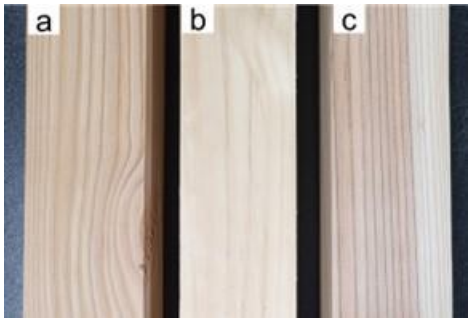

Fig. 1. Images of wood species (a- Japanese larch, b- Korean pine, and c- Japanese cedar)

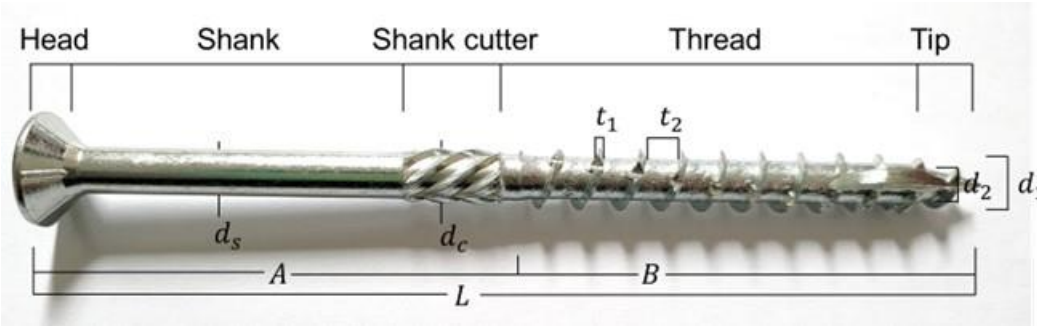

Fig. 2. Image of the STS

The fastener used galvanized carbon steel STS from Rothoblaas Corporation (Bozano, Italy). The 120 mm long STSs were divided into three groups by the diameters 8, 10, and 12 mm. The shank diameter (d_s) was 5.8, 7, and 8 mm, and the shank cutter diameter (d_c) was 6.8, 8.4, and 9 mm. The thread has an inner diameter d_2 and an outer diameter d_1.

Methods

Preparation of half-hole embedment strength specimens

The embedment strength specimens were cut to 50 × 50 mm^2 according to KS F 2156 (2022), and the three sections according to embedment loading directions, *i.e.*, the longitudinal section (L), the radial section (R), and the tangential section (T), were clearly distinguished (Fig. 4). The specimens were pressed with a clamp so that they faced two identical longitudinal sections, and a pre-hole with a diameter d_s (6, 7, and 8 mm) was provided at the center of the opposite longitudinal section (Fig. 3-a).

The grooved specimens were threaded into each piece by inserting and removing STSs (10, 11, and 12 mm) appropriate for the diameter (Fig. 3-b). Figure 3-c shows a threaded shape with a semicircular groove on the wood to be tested for embedment strength. The embedment strength test piece is divided into a T-series embedded with the thread of the STS and an S-series embedded with the shank. However, when the STS is inserted, a thread length is processed in the shank part; thus, both series process the thread path (Fig. 4). The specimen was named according to the tree species, each section, and the diameter of the STS (d_1), 8, 10, and 12 mm, and the location of the STS (thread and shank), as shown in Table 2. The STS with a diameter of 12 mm was not tested because the length of the shank was 40 mm, which was shorter than the length of the specimen. A total of 450 specimens were prepared, with 10 specimens for each type.

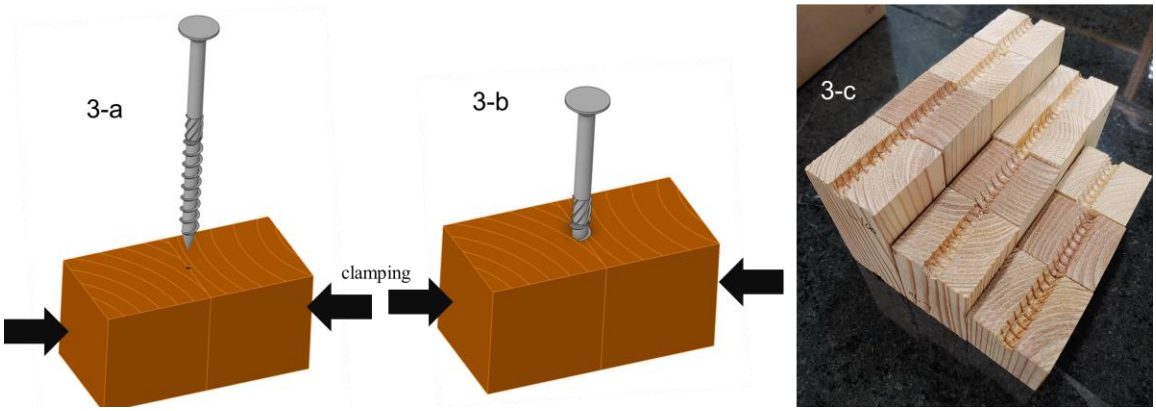

Fig. 3. Process of making an embedment specimen (a- clamping, b- drilling, and c- specimens)

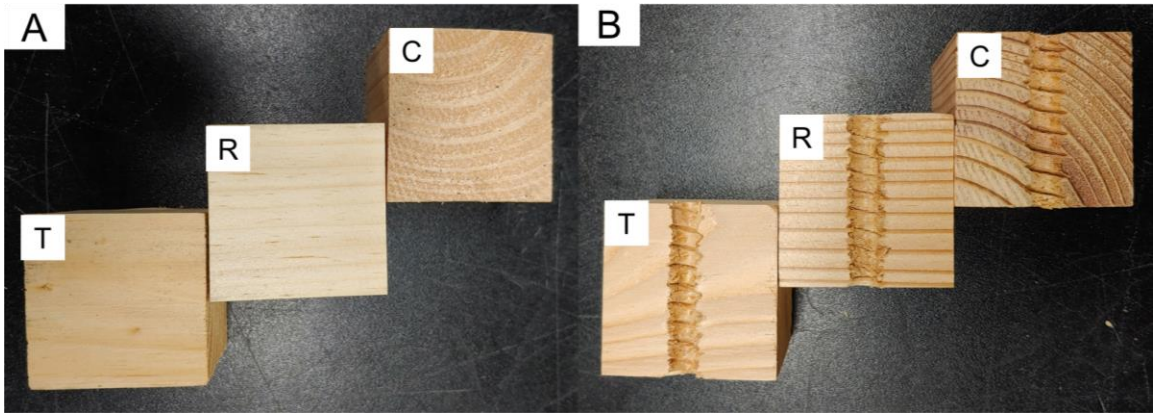

Fig. 4. Embedment section of the specimens on grain direction (A- before drilling the half-hole, B- after drilling the half-hole)

Table 2. Types of Specimens and Nomenclature

Species	Gain Directions	Thread and Tip			Shank and Shank Cutter	
		8 mm	10 mm	12 mm	8 mm	10 mm
Larix kaempferi (Lamb.) Carriere	Longitudinal section	LC8T	LC10T	LC12T	LC8S	LC10S
	Radial section	LR8T	LR10T	LR12T	LR8S	LR10S
	Tangential section	LT8T	LT10T	LT12T	LT8S	LT10S
Pinus koraiensis	Longitudinal section	KC8T	KC10T	KC12T	KC8S	KC10S
	Radial section	KR8T	KR10T	KR12T	KR8S	KR10S
	Tangential section	KT8T	KT10T	KT12T	KT8S	KT10S
Cryptomeria japonica	Longitudinal section	CC8T	CC10T	CC12T	CC8S	CC10S
	Radial section	CR8T	CR10T	CR12T	CR8S	CR10S
	Tangential section	CT8T	CT10T	CT12T	CT8S	CT10S

Test methods

For Japanese larch, Korean pine, and Japanese cedar specimens, specific gravity and annual ring width were measured after maintaining the equilibrium moisture content at constant temperature and humidity (25 °C and 65% humidity) for approximately one week. The T-series was tested by inserting only the threaded part into the groove, except for the tip part. The S-series was tested after the STS was inserted into the groove, including the shank and shank cutter. A compressive load was applied to the specimens at a rate of 0.5 mm/min using the load cell of Instron 5585 (debris-shield for floor-mounted testing machines, Norwood, USA) (Fig. 5). The load and cross-head movement were measured. The test was performed in accordance with the KS F 2156 (2022).

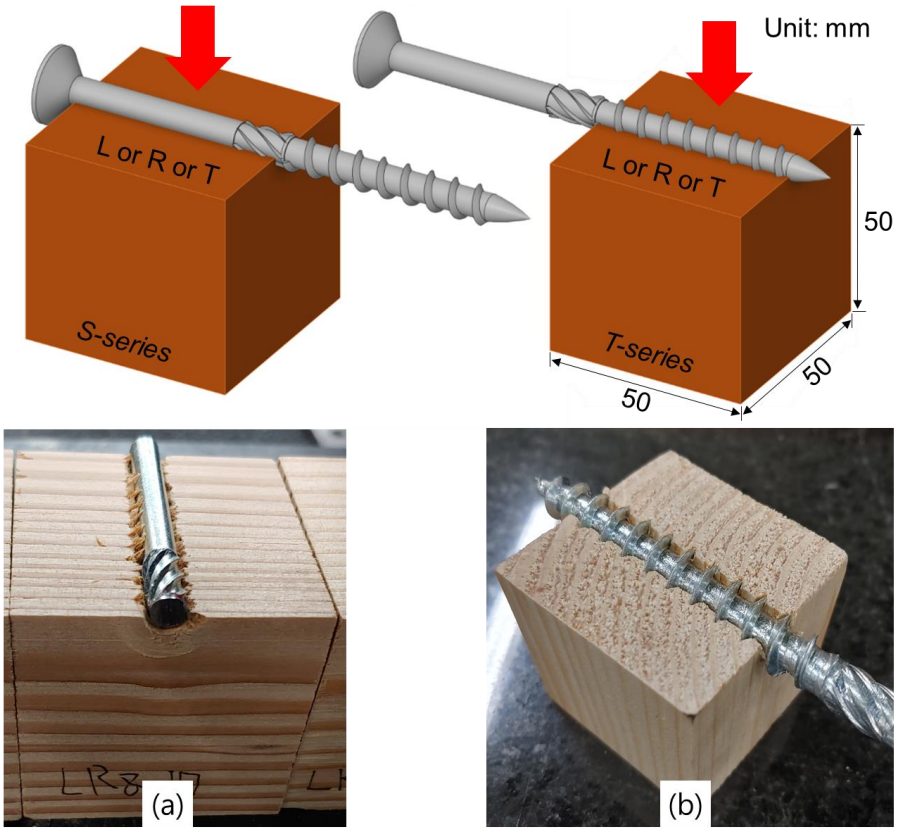

Fig. 5. Configuration of the embedment strength test specimen (a- S-series, b- T-series)

The maximum load of the wood longitudinal-section specimens is easy to measure because of the clear load drop, but the maximum load of the radial- and tangential-section specimens is difficult to measure because the load drop is not clear. Therefore, the embedment strength was calculated jointly as the yield strength, and the results were compared and analyzed.

The yield strength was calculated considering a 5% offset of the thread diameter of the STS fastener, according to KS F 2156 (2022). First, the initial straight line of the load–deformation curve obtained in the experiment was shifted in a parallel manner by 5% of the STS diameter, as shown in Fig. 6. Then, the yield load way was calculated at the intersection of the moved straight line and the load–deformation curve.

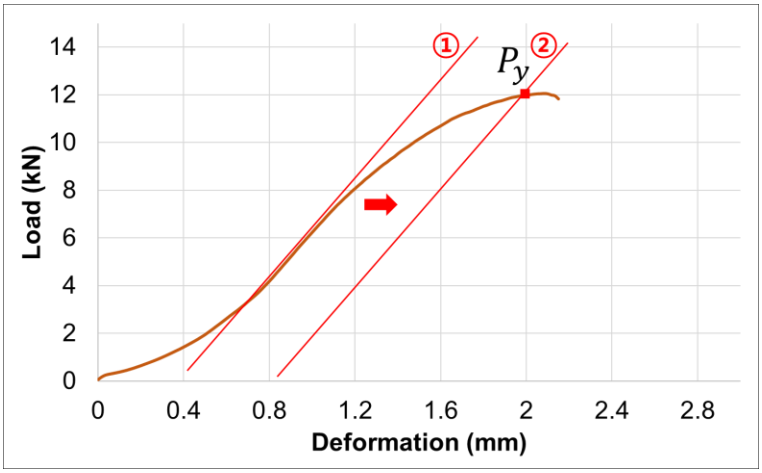

Fig. 6. Load–deformation curve at 5% offset yield load

The embedment strength was calculated by dividing the yield load by the projection area of the part of STS embedment to the timber specimens. The embedment strength was calculated in two types by varying the effective embedment area. Type 1 embedment strength was calculated by applying the embedment area based on the nominal diameter of the STS.

Type 1 embedment strength (B_{T1}, B_{S1}) was calculated according to Eqs. 1 to 4,

$$B_{T1} = P_y/A_{T1}, \quad (1)$$

$$B_{S1} = P_y/A_{S1}, \quad (2)$$

$$A_{T1} = L_t \times d_1, \quad (3)$$

$$A_{S1} = (a_s + a_c) \times d_s, \quad (4)$$

where B_{T1} is the type 1 STS thread part embedment strength (MPa), B_{S1} is the type 1 STS shank and shank cutter part embedment strength (MPa), P_y is the 5% offset embedment load (N), A_{T1} is the type 1 thread part embedment strength area (mm^2), A_{S1} is the type 1 shank and shank cutter part embedment strength area (mm^2), L_t is the thread length (mm), d_1 is the outside diameter of the thread (mm), a_s is the STS shank length (mm), a_c is the STS shank cutter length (mm), and d_s is the STS shank diameter (mm).

For Type 2, based on the exact measurement of the STS, the embedment strength of the effective embedment area was applied as the actual area as follows. For the S-series, the effective embedment area was determined by applying different diameters of the shank and shank cutter, and for T-series, the effective embedment area was applied by calculating the area of the thread. The height of a thread was calculated by dividing the difference between outer and inner diameters by two ($(d_1 - d_2)/2$).

Type 2 embedment strength (B_{T2}) was calculated according to Eqs. 5 to 8,

$$B_{T2} = P_y/A_{T2}, \; B_{S2} = P_y/A_{S1}, \quad (5)$$

$$A_{T2} = [t_1\{(d_1-d_2)/2 + d_2\} + (t_2 d_2)]/(t_1+t_2) \times L_t, \quad (6)$$

$$A_{S2} = a_s \times d_s + a_c \times d_c, \quad (7)$$

where B_{T2} is the type 2 STS Thread part embedment strength (MPa), A_{T2} is the type 2 thread embedment strength area (mm^2), A_{S2} is the type 2 shank and shank cutter part embedment strength area (mm^2), B_{S2} is the type 2 STS shank and shank cutter part embedment strength

(MPa), d_c is the STS shank cutter diameter (mm), t_2 is the d_2 length (mm), d_1 is the outer diameter of the thread, d_2 is the inner diameter of the thread (mm), and L_t is the embedment length of T-series (mm).

RESULTS AND DISCUSSION

Five Percent Offset Yield Load by Grain Direction of Softwood Species

The difference between the bearing stress in different orthogonal directions, wood species, and screw diameter was determined. The difference between the bearing stress for thread and shank screw diameter was also determined. Table 3 shows the average yield load of softwood with STS. The average yield load by tree species was calculated as 6.01 kN for Japanese larch, 5.47 kN for Korean pine, and 4.15 kN for cedar, with the yield load decreasing in the order of Japanese larch, Korean pine, and cedar. A higher specific gravity of the species resulted in a higher yield load.

Table 3. Five % Offset Yield Load for Grain Direction of Softwood Depending on the Type of STS

Species		Japanese Larch			Korean Pine			Japanese Cedar			
Grain Direction		L	R	T	L	R	T	L	R	T	Mean (MPa)
8T	mean	8.26	4.69	4.78	7.65	4.17	3.63	5.83	2.57	2.77	4.93
	CV	0.1	0.11	0.07	0.11	0.15	0.13	0.14	0.22	0.12	0.13
8S	mean	7.63	4.82	4.09	7.41	3.61	3.43	5.9	2.95	2.50	4.70
	CV	0.11	0.17	0.08	0.12	0.12	0.14	0.07	0.14	0.12	0.12
10T	mean	8.99	4.63	4.48	8.59	4.75	3.9	7.15	2.98	2.78	5.36
	CV	0.66	0.1	0.1	0.2	0.19	0.04	0.13	0.17	0.12	0.19
10S	mean	7.31	4.72	3.67	7.74	4.29	4.02	6.95	3.18	3.09	5.00
	CV	0.11	0.21	0.13	0.11	0.17	0.12	0.17	0.12	0.12	0.14
12T	mean	11.88	5.39	4.80	10.2	4.19	4.44	7.42	3.27	2.94	6.06
	CV	0.07	0.21	0.12	0.11	0.28	0.12	0.11	0.12	0.17	0.15
Mean (MPa)		8.81	4.85	4.36	8.32	4.20	3.88	6.65	2.99	2.82	
CV		0.10	0.11	0.07	0.11	0.15	0.13	0.14	0.22	0.12	

***** CV (coefficient of variation): standard deviation/mean

The average yield load of the longitudinal section was the highest in all directions at 7.93 kN, the radial section was 3.69 kN, and the tangential section had the lowest yield load at 4.01 kN. The average coefficient of variation was 0.18, 0.14, and 0.18, respectively, and the reliability of the value was high.

The loading and grain directions are parallel for the longitudinal section. Therefore, the resistance to the embedment load can be assumed to be large. This trend is similar to that reported in structural glulam (Kim and Hong 2008).

According to STS type, the average yield load tended to increase with increasing diameter, and the T-series had a higher average yield load than the S-series. The average yield load of the 8T specimens was 4.97 kN, the average yield load of the 8S specimens was 4.66 kN, the average yield load of the 10T specimens was 5.36 kN, the average yield load of the 10S specimens was 4.99 kN, and the average yield load of the 12T specimens was the highest at 6.06 kN.

Most of the failure modes of the specimens for embedment strength showed that the specimens were slightly embedded, and some of the specimens for embedment on the shank part were concentrated under the influence of the shank cutter, resulting in short cleavage. This is the same result as the failure mode for each direction of the pine wood in a previous study (Lee *et al.* 2022).

Calculation of embedment strength using the effective area of STS

Table 4 shows the results of embedment strength type 1. Table 5 shows the results of embedment strength type 2. The T-series showed increased embedment strength of type 2 by 40% to 54% compared to type 1, and the S-series showed the embedment strength of type 2 to be 3% to 4% lower than that of type 1. This seems to be due to the different embedment effective areas. For the T-series, the area between the thread and d_2 is subtracted, and the effective area of the embedment is reduced, improving the embedment strength. For the S-series, the area of the shank cutter, which is slightly thicker than the shank, was applied. The difference is large between the embedment strength calculated using only the outer diameter and the embedment strength considering the effective area of the embedment in more detail. Therefore, the embedment strength of type 2 was used as the basis for the comparative embedment strength verification.

Table 4. Average Embedment strength Type 1 of Softwood Measured with STS

Species	Japanese larch (MPa)			Korean pine (MPa)			Japanese cedar (MPa)			Mean (MPa)	CV
Grain Direction	L	R	T	L	R	T	L	R	T		
8T	20.6	12.0	11.7	19.1	9.1	10.4	14.6	6.9	6.4	12.5	0.37
8S	26.3	14.1	16.6	25.5	11.8	12.4	20.3	8.6	10.2	16.4	0.36
10T	18.0	9.0	9.3	17.2	7.8	9.5	14.3	5.6	6.0	10.9	0.39
10S	20.9	10.5	13.5	22.1	11.5	12.3	19.9	8.8	9.1	14.2	0.34
12T	14.1	5.7	6.4	12.2	5.3	5.0	8.8	3.5	3.9	7.4	0.45
Mean (MPa)	20.0	10.3	11.5	19.2	9.1	9.9	15.6	6.7	7.1		
CV	0.20	0.28	0.30	0.24	0.27	0.27	0.27	0.30	0.32		

***** CV (coefficient of variation): standard deviation/mean

Table 5 lists the results of the calculation of the embedment strength according to the above equations (Eq. 5). The average embedment strength according to the wood species is as follows. Japanese larch and Korean pine were measured as 19.77 MPa and 18.47 MPa, respectively, and cedar had the lowest average embedment strength with an average of 15.57 MPa.

The embedment strength along the grain direction was as follows. The embedment strength of the longitudinal section of Japanese larch was the highest at 26.3 MPa, and that of the radial section of cedar was the lowest at 9.2 MPa. All species had the highest embedment strength in the longitudinal section, and the embedment strengths in the radial and tangential sections were similar.

Figure 7 shows the results of the regression analysis of the specific gravity and embedment strength of Japanese larch, Korean pine, and Japanese cedar. The embedment strengths of the longitudinal, radial, and tangential sections showed significant trends with R^2 values of 0.31, 0.51, and 0.53, respectively. The embedment strength of the representative species of softwood structural materials in Korea increased in proportion to the specific gravity. The specific gravity according to species and the embedment strength according to grain direction are considered the main factors in the equation for predicting embedment strength.

The embedment strength as a function of the STS shape was as follows. The threaded T-series showed higher embedment strength than the threaded S-series. This was the result of performing the embedment strength test on the preprocessed threaded specimens, and the embedment area of the T-series and STS is considered wider than that of the S-series.

Table 5. Average Embedment strength of Softwood Measured with STS

Species	Japanese Larch (MPa)			Korean Pine (MPa)			Japanese Cedar (MPa)			Mean (MPa)	CV
Grain Direction	L	R	T	L	R	T	L	R	T		
8T	28.93	16.8	16.4	26.8	12.7	14.6	21.3	10.1	9.4	18.6	0.11
8S	25.44	13.6	16.1	24.7	11.4	12.0	19.7	8.3	9.8	16.8	0.12
10T	26.23	13.1	13.5	25.0	11.4	13.8	24.2	9.4	10.1	17.1	0.12
10S	20.08	10.1	13.0	21.3	11.0	11.8	19.1	8.5	8.7	14.5	0.13
12T	30.66	12.4	13.9	26.3	11.5	10.8	24.1	9.6	10.7	16.8	0.14
Mean (MPa)	26.3	13.2	14.6	24.8	11.6	12.6	21.7	9.2	9.7		
CV	0.17	0.14	0.17	0.14	0.14	0.20	0.13	0.15	0.17		

***** CV (coefficient of variation): standard deviation/mean

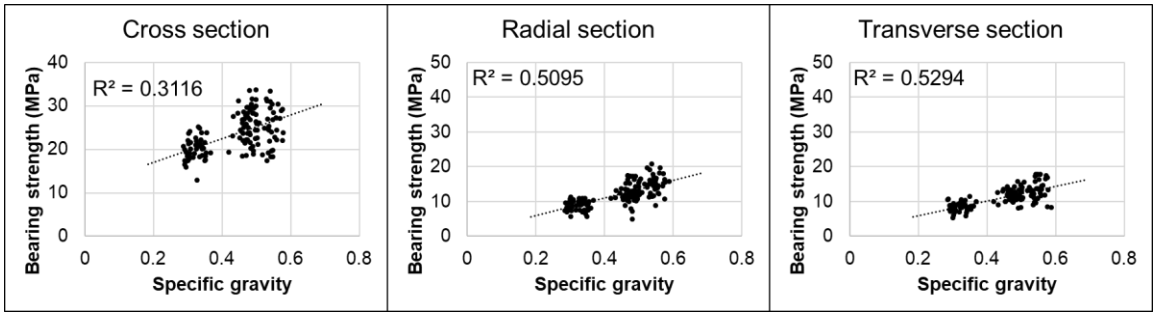

Fig. 7. Results of the regression analyses of the embedment strength and the specific gravity by grain direction of the timber

Table 6 lists the results of the calculation of the embedment strength ratio parallel and perpendicular to the grain. For the embedment strength ratio by wood species, the Japanese larch was the highest, within the range 0.43 to 0.58. Higher specific gravity is considered to have resulted in lower embedment strengths perpendicular to the grain than the embedment strength parallel to the grain. Depending on the STS type, a smaller diameter resulted in increased embedment strength perpendicular to the grain. For the NDS standard, the load-embedment strength is calculated by multiplying the adjustment factor when the direction of the embedment load is at an angle to the grain direction of the members. Therefore, the embedment strength ratio for grain direction on the tree species obtained through the embedment test can be an adjustment factor for the predicted embedment strength required to predict the strength according to the grain direction of the STS connection.

Table 6. Embedment Strength of Experimental Values According to Tree Species and Grain Direction

Species	Japanese Larch			Korean Pine			Japanese Cedar		
Grain Direction	$F_{\parallel}$	$F_{\perp}$	$F_{\perp}/F_{\parallel}$	$F_{\parallel}$	$F_{\perp}$	$F_{\perp}/F_{\parallel}$	$F_{\parallel}$	$F_{\perp}$	$F_{\perp}/F_{\parallel}$
8T	28.9	16.6	0.57	26.8	13.7	0.51	20.4	9.4	0.46
8S	25.4	14.9	0.58	24.7	11.7	0.47	19.7	9.1	0.46
10T	26.2	13.3	0.51	25	12.6	0.50	20.9	8.4	0.40
10S	20.1	11.5	0.57	21.3	11.4	0.54	19.1	8.6	0.45
12T	21.9	9.4	0.43	18.8	8	0.42	13.6	5.7	0.42
Mean	24.5	13.1	0.53	23.3	11.5	0.49	18.7	8.2	0.44
CV (%)	12.9	19.1	11.1	12.3	16.8	7.90	14.0	15.8	5.3

***** CV (coefficient of variation): standard deviation/mean

The experimentally calculated embedment strength parallel and perpendicular to the grain was compared and analyzed with the predicted embedment strength for lag screws calculated by NDS in North America, Eurocode 5 in Europe, and CSA in Canada (Fig. 8). To convert the unit of embedment strength proposed by NDS to MPa, the formula proposed by KDS was used. The prediction formula for the embedment strength of structural timber using fasteners applies to the equation, but the STS applied the average diameter because the threads have different spacings between pitches and pitch. The average diameter of the

STS was calculated using the value obtained by dividing the projection area d_t by the STS embedment length (50 mm). For 8T, 8S, 10T, 10S, and 12T, 5.7, 6, 6.9, 7.3, and 7.8 mm were used, respectively.

The embedment strength prediction was according to Eqs. 8 through 10,

$$\text{KDS: } F_{\parallel} = 79G,\ F_{\perp} = (216G^{1.45})/\sqrt{d}, \quad (8)$$

$$\text{Eurocode 5: } F_{\parallel} = 0.082(1\text{-}0.01d)G,\ F_{\perp} = \{0.082(1-0.01d)G\}/(1.35+0.015d), \quad (9)$$

$$\text{CSA: } F_{\parallel} = 28d^{-0.5}G^{0.56},\ F_{\perp} = 96d^{-0.5}G^{1.05}, \quad (10)$$

where $F_{\parallel}$ is the horizontal embedment strength (MPa), $F_{\perp}$ is the vertical embedment strength (MPa), G is the specific gravity (-), and d is the fastener diameter (mm).

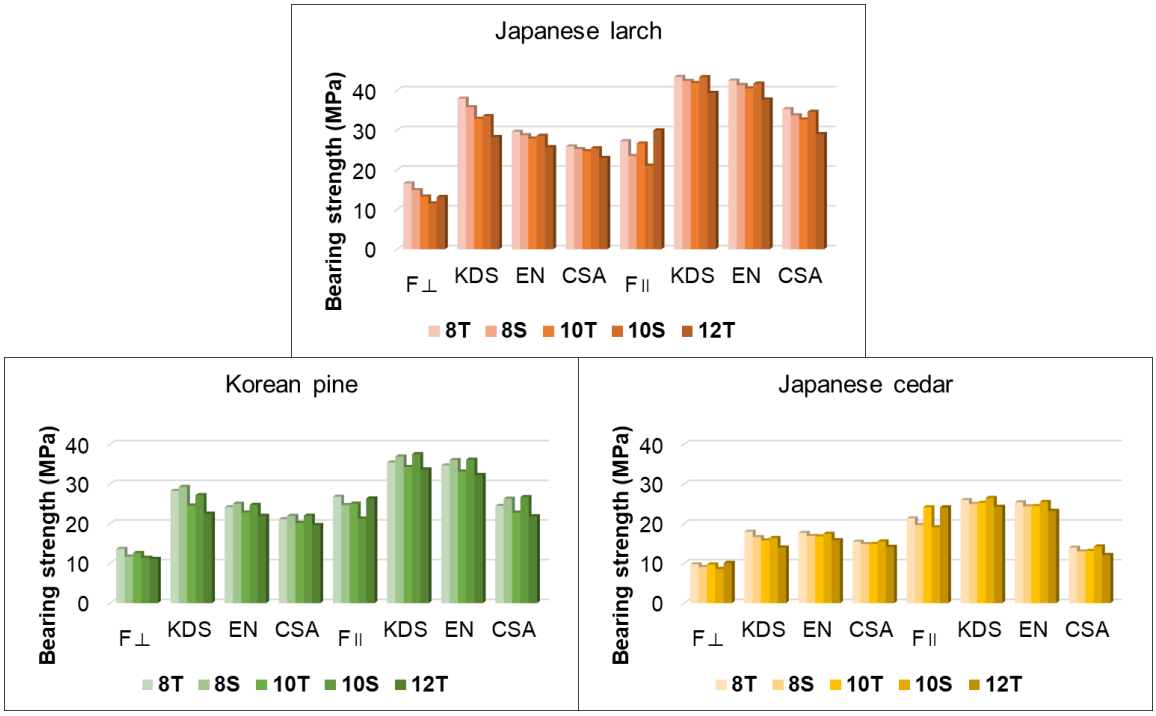

Fig. 8. Comparison of the results between the measured embedment strength and the predicted embedment strength using STS

The actual measured embedment strength using STS was mostly lower than the general fastener prediction equation (KDS, EN, and CSA) calculated using the diameter of the fastener and the specific gravity of wood. The strength ratio of the test specimens to which the load was applied in the vertical direction of the fiber was measured as 0.44, 0.48, and 0.48, in the order of KDS, EN, and CSA, respectively, and each material to which the load was applied in the parallel direction of the fiber was measured as 0.66, 0.68, and 0.68. The strength ratio of each species was 0.52 for Japanese larch, 0.57 for Korean pine, and 0.62 for Japanese cedar. The lower the proportion of Japanese cedar, the more similar the predicted embedment strength and the measured embedment strength were. Thus, the general equation for predicting fasteners shows a large deviation between 38% and 56% from the embedment strength of STS. When the embedment effective area was set in type 1, the difference was larger than the result of applying the embedment effective area to type 2.

Therefore, when using the method to predict the embedment strength of STS connections, the effective embedment area should be set according to the information concerning STS shape, and a suitable experimental equation is developed based on the density of members, the STS diameter and the loading direction.

ACKNOWLEDGMENT

This research was supported by a Research Project (FP0200-2021-01-2023) through the National Institute of Forest Science (NIFoS), Korea.

CONCLUSIONS

1. In this study, the embedment strength for each direction of Korean species was calculated using self-tapping screws (STS). The yield load of the 5% offset calculated by the embedment of the threaded part was higher than the yield load of the specimen embedment of the shank part.
2. The embedment strength was highest in a longitudinal section where the fiber direction and the loading direction were parallel, and the radial and tangential sections perpendicular to the fiber direction and the loading direction showed relatively low embedment strength performance.
3. The embedment strength (NDS, EN, and CSA) calculated by the fastener formula for calculating the effective area of embedment was not suitable, as it showed a difference of 38% to 56% in the embedment strength results using STS.
4. In future works, the prediction formula for embedment strength will be developed considering the adjustment factor based on the shape information of STS and proposed for the design lateral strength for cross-laminated timber (CLT) connections using STS fasteners.

REFERENCES CITED

Aloisio, A., Pasca, D., Tomasi, R., and Fragiacomo, M. (2020). "Dynamic identification and model updating of an eight-story CLT building," *Eng. Struct.* 213, article 110593. DOI: 10.1016/j.engstruct.2020.110593

Brandner, R. (2019). "Properties of axially loaded self-tapping screws with focus on application in hardwood," *Wood Mater. Sci. Eng.* 14(5), 254-268. DOI: 10.1080/17480272.2019.1635204

Brandner, R., Ringhofer, A., and Reichinger, T. (2019). "Performance of axially-loaded self-tapping screws in hardwood: Properties and design," *Eng. Struct.* 188, 677-699. DOI: 10.1016/j.engstruct.2019.03.018

Brown, J. R., Li, M., Tannert, T., and Moroder, D. (2021). "Experimental study on orthogonal joints in cross-laminated timber with self-tapping screws installed with mixed angles," *Eng. Struct.* 228, article 111560. DOI: 10.1016/j.engstruct.2020.111560

Dietsch, P., and Brandner, R. (2015). "Self-tapping screws and threaded rods as reinforcement for structural timber elements–A state-of-the-art report," *Constr. Build. Mater.* 97, 78-89. DOI: 10.1016/j.conbuildmat.2015.04.028

Fitzgerald, D., Sinha, A., Miller, T. H., and Nairn, J. A. (2021). "Axial slip-friction connections for cross-laminated timber," *Eng. Struct.* 228, article 111478. DOI: 10.1016/j.engstruct.2020.111478

Hossain, A., Popovski, M., and Tannert, T. (2019). "Group effects for shear connections with self-tapping screws in CLT," *J. Struct. Eng.* 145(8), article 04019068. DOI: 10.1061/(ASCE)ST.1943-541X.0002357

Jockwer, R., Steiger, R., and Frangi, A. (2014). "Fully threaded self-tapping screws subjected to combined axial and lateral loading with different load to grain angles," in: *Materials and Joints in Timber Structures*, pp. 265-272. DOI: 10.1007/978-94-007-7811-5_25

Khan, R., Niederwestberg, J., and Chui, Y. H. (2021). "Influence of insertion angle, diameter and thread on embedment properties of self-tapping screws," *Eur. J. Wood Wood Prod.* 79(3), 707-718. DOI: 10.1007/s00107-020-01651-5

Kim, K. H., and Hong, S. I. (2008). "Bearing properties of domestic *Larix glulam*," *J. Korean Wood Sci. Tech.* 36(4), 93-101.

Korea Forest Service 3020 (2018). *Statistical Yearbook of Forestry*, Daejeon, Republic of Korea.

Korean Standards Association. (2022). "Method of dowel-bearing strength test for wood and wood-based products," KS F 2156.

Lee, I. H., Kim, K., and Shim, K. B. (2022). "Evaluation of bearing strength of self-tapping screws according to the grain direction of domestic *Pinus densiflora*," *J. Korean Wood Sci. Tech.* 50(1), 1-11.

Li, X., Ashraf, M., Subhani, M., Ghabraie, K., Li, H., and Kremer, P. (2021). "Withdrawal resistance of self-tapping screws inserted on the narrow face of cross laminated timber made from radiata pine," *Structures* 31, 1130-1140. DOI: 10.1016/j.istruc.2021.02.042

Market Survey of Timber Products (2020). Korea Forest Service, Daejeon, Republic of Korea.

Mirdad, M. A. H., Jucutan, A., Khan, R., Niederwestberg, J., and Chui, Y. H. (2022). "Embedment and withdrawal stiffness predictions of self-tapping screws in timber," *Constr. Build. Mater.* 345, article 128394. DOI: 10.1016/j.conbuildmat.2022.128394

Mohammad, M., Blass, H., Salenikovich, A., Ringhofer, A., Line, P., Rammer, D., and Li, M. (2018). "Design approaches for CLT connections," *Wood Fiber Sci.* 27-47. DOI: 10.22382/wfs-2018-038

Nguyen, T. T., Dao, T. N., Aaleti, S., van de Lindt, J. W., and Fridley, K. J. (2018). "Seismic assessment of a three-story wood building with an integrated CLT-lightframe system using RTHS," *Eng. Struct.* 167, 695-704. DOI: 10.1016/j.engstruct.2018.01.025

Van de Lindt, J. W., Furley, J., Amini, M. O., Pei, S., Tamagnone, G., Barbosa, A. R., Rammer, D., Line, P., Fragiacomo, M., and Popovski, M. (2019). "Experimental seismic behavior of a two-story CLT platform building," *Eng. Struct.* 183, 408-422. DOI: 10.1016/j.engstruct.2018.12.079

Xu, J., Zhang, S., Wu, G., Gong, Y., and Ren, H. (2021). "Withdrawal properties of self-tapping screws in Japanese larch (*Larix kaempferi* (Lamb.) Carr.) cross laminated timber," *Forests* 12, article 524. DOI: 10.3390/f12050524

Article submitted: November 2, 2023; Peer review completed: February 11, 2023;
Revised version received and accepted: March 18, 2023; Published: April 3, 2023.
DOI: 10.15376/biores.18.2.3576-3589